Characterization of Some Novel First Row Transition Metal Carbonyl Chlorides by Infrared and EXAFS Spectroscopy of Matrix-Isolated Species

Ian R. Beattie,* Peter J. Jones, and Nigel A. Young

Contribution from the Chemistry Department, The University of Southampton, Southampton SO9 5NH, U.K. *Received November 26, 1991*

Abstract: The isolation of the dichlorides of Ca, Cr, Mn, Fe, Co, Ni, and Zn in argon matrices doped with ca. 1% carbon monoxide results in a ν_{CO} feature shifted to *high* frequency of "free" CO. In two cases (Cr and Fe) annealing caused the formation of carbonyl halides with ν_{CO} at 2096 and 2110 cm^{-1}, respectively. When the dichlorides were isolated in pure CO matrices (or argon matrices which were highly enriched in CO), in all cases *except* Ca (d^0), Mn (d^5), and Zn (d^{10}), carbonyl halides were formed. This was demonstrated by the use of isotopic substitution and infrared spectroscopy to identify δ_{MCO} and (in several cases) ν_{M-C} modes. The use of isotopic and partial isotopic substitution (^{13}CO; $C^{18}O$) enabled the complete identification of *trans*-$[Fe(CO)_4Cl_2]$. EXAFS data are fully in agreement with the formulation and give the following distances: Fe-C, 1.85 (3) Å; Fe-O, 2.96 (4) Å; Fe-Cl, 2.25 (3) Å. On the basis of combined infrared and EXAFS data, *trans*-$[Cr(CO)_4Cl_2]$ is also characterized. The following bond lengths were obtained: Cr-C, 2.00 (3) Å; Cr-O, 3.11 (5) Å; Cr-Cl, 2.27 (3) Å. For $CoCl_2$ and $NiCl_2$, the spectra are complicated by the presence of more than one species in the matrix, so that EXAFS data were not of assistance. In both cases, metal carbonyl halides were formed and isotopic substitution coupled with ν_{M-Cl} frequencies led to the suggestion that the major species are *trans*-$[Ni(CO)_2Cl_2]$ and *trans*-$[Co(CO)_4Cl_2]$.

1. Introduction

Matrix isolation represents a unique approach to the study of the interaction of individual molecules, radicals, or ions with a surrounding host. In essence, it can be used as a technique for studying the behavior of otherwise inaccessible species in (solid) solutions ranging from inert gases through nitrogen and carbon monoxide to more conventional solvents such as HCN or acetonitrile. We have already published research on the behavior of some first row transition element dichlorides in nitrogen.[1] Perhaps the most surprising aspect of this work was the nonlinearity of the later members, notably $NiCl_2$ with a bond angle of about 130° (derived from isotopic shift data). This is in sharp contrast to the normally assumed linearity of the first row transition element dichlorides in the gas phase.[2] The present paper extends the earlier work in nitrogen by using the isoelectronic molecule carbon monoxide.

Carbon monoxide can interact with molecular halides in a variety of ways. For the monomeric species with terminal CO ligands these interactions range from van der Waals interactions as found in trigonal $BF_3 \cdot CO$[3] to strong bonding interactions in species such as linear AuCl·CO[4] or octahedral *cis*-$[Fe(CO)_4Cl_2]$.[5] It is well established that many metal halides isolated in cryogenic matrices can interact with dopant carbon monoxide to give species with ν_{CO} shifted to *high* frequency of "free" carbon monoxide. These studies include the difluorides of chromium, manganese, nickel, copper, and zinc and also nickel dichloride.[6] In addition, dihalides of tin and lead,[7] of mercury,[8] and of the alkaline earth metals;[9] halides of the lanthanides;[9] and uranium tetrafluoride[10] have been studied, notably in the ν_{CO} region. Hauge et al.[9] have summarized much of this work and also attempted to correlate the following: the shift in ν_{CO} of the "1:1 complex" from that of free CO with the *formal* metal charge divided by the square of the "metal to CO distance". A similar approach has been used for CO on metal oxide surfaces.[11] However, it is important to recall that bonding CO to a metal (or other) center causes an increase in frequency purely due to kinematic effects without any necessary change in the CO force constant.

For three of the first row transition metals, there are well-established monomeric carbonyl halides: $[Cr(CO)_5I]$, $[Mn(CO)_5X]$, and *cis*-$[Fe(CO)_4X_2]$ where X = Cl, Br, or I. (The synthesis of the trans form of $[Fe(CO)_4I_2]$ has also been reported.[12]) It has been shown that annealing a matrix of $FeCl_2$ isolated in argon doped with carbon monoxide leads to dramatic changes in the infrared spectrum,[13] with the formation of *trans*-$[Fe(CO)_4Cl_2]$.

In this paper, we report a study of Ca, Cr, Mn, Fe, Co, Ni, and Zn dichlorides isolated in matrices of argon doped with carbon monoxide or in pure carbon monoxide.

2. Strategy

The primary physical technique for these studies was infrared spectroscopy of the species isolated in the matrix, covering the frequency range 4000-200 cm^{-1}. Isotopic substitution (^{13}CO, $C^{18}O$, or ^{37}Cl) was used to characterize ν_{M-C}, δ_{MCO}, and ν_{M-Cl} modes. Where appropriate, additional EXAFS studies were carried out.

Most of the vibrational modes that are expected to occur above 200 cm^{-1} are easily visualized (ν_{CO}, ν_{M-C}, and ν_{M-Cl}). However, the δ_{MCO} modes require some comment. Assuming the M-C-O bonds to be linear, δ_{MCO} may be represented by a transition dipole perpendicular to the M-C-O direction. The primary movement in the δ_{MCO} vibration is that of the lightest atom (carbon), and indeed these deformations can be considered as librations of a CO molecule in the field of the metal ion. Their intensity is thus largely defined by the (square of the) *permanent* dipole of the carbonyl group, together with any enhancement due to coupling with vibrations of suitable symmetry which occur in a similar region of the spectrum (e.g., ν_{M-Cl}). Clearly, major shifts in frequency will occur for $^{12}C/^{13}C$ isotopic substitution as the major movement is concentrated on the light carbon atom (the $^{16}O/^{18}O$ shifts being smaller).

By contrast, in the ν_{M-C} modes, the CO may crudely be regarded as a point mass so that in this case, for $^{16}O/^{18}O$ substitution, the

(1) Beattie, I. R.; Jones, P. J.; Young, N. A. *Chem. Phys. Lett.* **1991**, *177*, 579-584. Beattie, I. R.; Jones, P. J.; Young, N. A. *Mol. Phys.* **1991**, *72*, 1309-1312.
(2) Hargittai, M.; Subbotina, N. Y.; Kolonits, M.; Gershikov, A. G. *J. Chem. Phys.* **1991**, *94*, 7278-7286.
(3) Janda, K. C.; Bernstein, L. S.; Steed, J. M.; Novick, S. E.; Klemperer, W. *J. Am. Chem. Soc.* **1978**, *100*, 8074-8079.
(4) Jones, P. G. *Z. Naturforsch.* **1982**, *B37*, 823-824.
(5) Noack, K. *Helv. Chim. Acta* **1962**, *45*, 1847-1859.
(6) Van Leirsburg, D. A.; DeKock, C. W. *J. Phys. Chem.* **1974**, *78*, 134-142. DeKock, C. W.; Van Leirsburg, D. A. *J. Am. Chem. Soc.* **1972**, *94*, 3235-3237.
(7) Tevault, D.; Nakamoto, K. *Inorg. Chem.* **1976**, *15*, 1282-1287.
(8) Tevault, D.; Strommen, D. P.; Nakamoto, K. *J. Am. Chem. Soc.* **1977**, *99*, 2997-3003.
(9) Hauge, R. H.; Gransden, S. E.; Margrave, J. L. *J. Chem. Soc., Dalton Trans.* **1979**, 745-748.
(10) Kunze, K. R.; Hauge, R. H.; Margrave, J. L. *J. Phys. Chem.* **1977**, *81*, 1664-1667.
(11) See, for example: Zaki, M. I.; Knözinger, H. *Spectrochim. Acta* **1987**, *43A*, 1455-1459.
(12) Pańkowski, M.; Bigorgne, M. *J. Organomet. Chem.* **1969**, *19*, 393-398.
(13) Beattie, I. R.; McDermott, S. D.; Mathews, E. A.; Millington, K. R.; Willson, A. D. *Angew. Chem., Int. Ed. Engl.* **1988**, *27*, 1161-1162.

0002-7863/92/1514-6146$03.00/0

Table I. Infrared Active δ_{MCO}, ν_{M-C} and ν_{M-Cl} Vibrations

compd	point group	vibration[a]	symmetry[b]
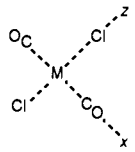	D_{2h}	δ_{MCO} op	b_{2u}
		δ_{MCO} ip	b_{1u}
		ν_{M-C}	b_{3u}
		ν_{M-Cl}	b_{1u}
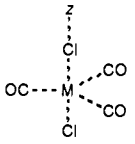	D_{3h}	δ_{MCO} op	a_2''
		δ_{MCO} ip	e'
		ν_{M-C}	e'
		ν_{M-Cl}	a_2''
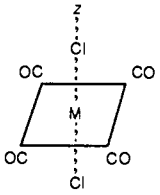	D_{4h}	δ_{MCO} op	a_{2u}
		δ_{MCO} ip	e_u
		ν_{M-C}	e_u
		ν_{M-Cl}	a_{2u}

[a] In plane = ip; out of plane = op. [b] Dotted lines indicate that coupling is symmetry allowed.

Table II. Effects of Isotopic Substitution (E.g., ^{13}CO) on e' (D_{3h}) and e_u (D_{4h}) δ_{MCO} Modes Assuming a ^{12}CO:^{13}CO Ratio of 1:1

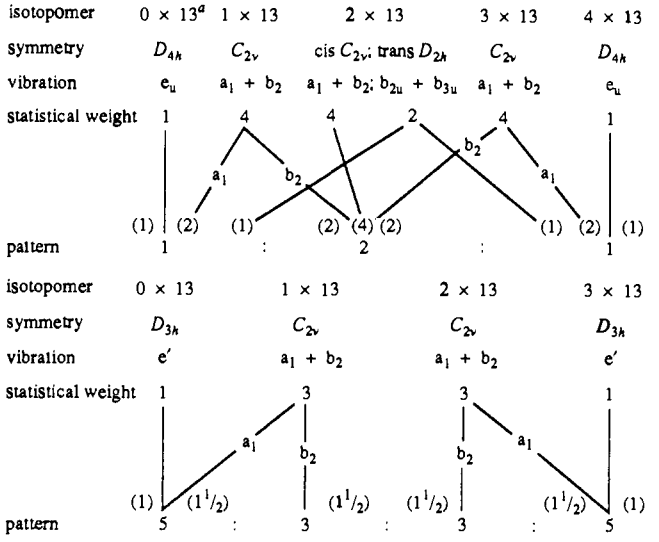

[a] 1 × 13 implies $(^{13}CO)(^{12}CO)_3$ for D_{4h}.

change in frequency is *greater* than that for $^{12}C/^{13}C$ substitution. Note also that ν_{CO} modes are of the same symmetry as ν_{M-C} modes. It is also important to realize that *partial* isotopic substitution can lead to lowering of symmetry and hence infrared activity of otherwise inactive bands. Further, frequency and intensity patterns of bands from partially substituted isotopomers can be affected due to coupling with other vibrations of appropriate symmetry, leading to distributions which are different from those which are intuitively expected.

In Table I we summarize the infrared active modes δ_{MCO}, ν_{M-C}, and ν_{M-Cl} for D_{2h} [$M(CO)_2Cl_2$], D_{3h} [$M(CO)_3Cl_2$], and D_{4h} [$M(CO)_4Cl_2$]. (In all cases, a linear MCl_2 unit is assumed.) In the absence of coupling, the effect of 1:1 isotopic substitution (^{12}CO:^{13}CO or $C^{16}O$:$C^{18}O$) on nondegenerate infrared active δ_{MCO} modes is that each band of the parent molecule appears as a symmetrical multiplet corresponding to the number of carbonyl groups plus 1, with the expected binomial distribution. Thus for D_{3h} [$M(CO)_3Cl_2$] the a_2'' mode would yield a 1:3:3:1 quartet. However, where a degeneracy is present (as in D_{3h} e' or D_{4h} e_u modes), the situation is less clear cut, and indeed for D_{4h} symmetry this approach yields a triplet (see Table II), as found for (nondegenerate) D_{2h} [$M(CO)_2Cl_2$]. Thus unless the nondegenerate modes can be identified for D_{4h} species, the number of carbonyl groups is not established unambiguously by this technique. For a D_{3h} parent molecule, applying statistical abundance and descent of symmetry to the various isotopomers leads to a quartet, but with an unusual intensity distribution, namely, 5:3:3:5. (In using Table II, it is important to remember that introduction of one different isotope (^{13}C or ^{18}O) defines the C_2 axis of the "new" molecule and removes any degeneracy present in the original molecule. Similarly, some care is necessary in using character tables because of an axis switch in going from, e.g., D_{4h} to C_{2v}.)

3. Results

These are difficult and time-consuming experiments. Precise duplication in two apparently identical experiments is almost impossible so that spectra with ^{12}CO, ^{13}CO, $C^{18}O$, $M^{35}Cl_2$, and $M^{37}Cl_2$ will not necessarily be amenable to subtraction routines, for example. The bands in the low-frequency region are weak for CO species, and spectra in pure carbon monoxide matrices (unlike those in nitrogen) do not show $^{35}Cl/^{37}Cl$ isotope fine structure, presumably because CO is an asymmetric molecule in terms of polarity and size. Annealing not only will cause interaction with dopants or the matrix but may also lead to polymer formation by the metal dihalides.[14] These polymers may then react further with dopants or the matrix. Finally, it is well-known that even in reactive matrices there may be "isolated" species which behave as if the matrix is inert.[15]

A. Carbon Monoxide Doped Matrices. When the first row transition element dichlorides $CrCl_2$ to $ZnCl_2$ inclusive were isolated in argon matrices doped with carbon monoxide (argon:CO ratio 100:1 to 1000:1), sharp bands shifted to high frequency of "free" CO were observed. ($TiCl_2$ and VCl_2 were not examined because of extensive disproportionation.[16,17] In the case of $CaCl_2$, the only band observed was broad and the frequency of 2186 cm^{-1} is open to question.) On a statistical basis, at these concentrations, less than one MCl_2 molecule in 10 will have an adjacent ("equatorial") carbon monoxide molecule to interact with. In agreement with earlier literature[9] we assume that where more than one ν_{CO} mode of a "complex" is observed, the *highest* frequency component corresponds to MCl_2 interacting with one CO molecule. The results obtained were as follows: $CrCl_2$, 2188 cm^{-1} (triplet); $MnCl_2$, 2194 cm^{-1}; $FeCl_2$, 2175 cm^{-1}; $CoCl_2$, 2192 cm^{-1}; $NiCl_2$[6], 2189 cm^{-1}; $ZnCl_2$, 2188 cm^{-1}. For these matrices which were not annealed, the small variations in the ν_{CO} modes (maximum difference 19 cm^{-1} in ca. 2200 cm^{-1}) are probably not significant.

In two instances (Cr and Fe) annealing at ca. 27 K caused major changes in the spectra, in each case giving one intense ν_{CO} mode in the region of 2100 cm^{-1} (2096 and 2110 cm^{-1}, respectively), suggesting the formation of carbonyl halides with *trans* chlorines. (In the case of $CrCl_2$ there was a weak band at 2053 cm^{-1} which we did not assign.) Unfortunately, in experiments using 1:1 mixtures of ^{12}CO and ^{13}CO or $C^{16}O$ and $C^{18}O$ we were not able to determine the number of CO molecules coordinated to the central atom.[18] The bands of "free" ^{13}CO or $C^{18}O$ occur in the same regions as ν_{CO} for $^{12}C^{16}O$ in these two metal carbonyl halides.

When interpreting spectra in the ν_{CO} region, it is important to note the following: (a) that lower frequency bands tend to be much more intense than those at higher frequency,[19] (b) that allowing CO to interact with a (heavy) metal center results in a kinematic effect, and (c) that bands due to species such as $CO{\cdot}H_2O$,[20] $CO{\cdot}HCl$,[21] and polymers of CO[22] obscure regions of the spectrum close to "free" CO.

(14) (a) Thompson, K. R.; Carlson, K. D. *J. Chem. Phys.* **1968**, *49*, 4379–4384. (b) Frey, R. A.; Werder, R. D.; Günthard, H. H. *J. Mol. Spectrosc.* **1970**, *35*, 260–284.
(15) Doeff, M. M.; Parker, S. F.; Barrett, P. H.; Pearson, R. G. *Inorg. Chem.* **1984**, *23*, 4108–4110.
(16) Hastie, J. W.; Hauge, R. H.; Margrave, J. L. *High Temp. Sci.* **1971**, *3*, 257–274.
(17) Beattie, I. R.; Jones, P. J.; Willson, A. D.; Young, N. A. *High Temp. Sci.* **1990**, *29*, 53–62.
(18) Darling, J. H.; Ogden, J. S. *J. Chem. Soc., Dalton Trans.* **1972**, 2496–2503.

Table III. Infrared Data[a] for Metal Dichlorides Isolated in Carbon Monoxide Matrices

species	$^{12}C^{16}O$	$^{12}C^{16}O/^{13}C^{16}O$	$^{13}C^{16}O$	$^{12}C^{18}O$	^{37}Cl	assignment
trans-$[Cr(CO)_4Cl_2]$	533.8 (s)		518.3 (s)	530.4 (s)	532.4 (s)	δ_{M-C-O}
	530.2 (sh)		516.3 (sh)	529.2 (sh)		δ_{M-C-O}
	384.3 (s)		378.8 (s)	383.4 (s)	378.2 (s)	ν_{M-Cl} (a_{2u})
	351.4 (m)		347.0 (m)	345.9 (m)	353.8 (m)	ν_{M-C} (e_u)
trans-$[Fe(CO)_4Cl_2]$	606.6 (s)	603.2 599.5 595.6	591.4 (s)	604.4 (s)		δ_{M-C-O} (a_{2u})
	582.3 (s)	582.6 575.6 567.3	566.7 (s)	580.1 (s)		δ_{M-C-O} (e_u)
	387.0 (m)	385.5 (m)	385.0 (m)	387.2 (m)		ν_{M-Cl} (a_{2u})
	380.4 (m)	378.5 (m)	375.0 (m)	373.8 (m)		ν_{M-C} (e_u)
$CoCl_2/CO$	518.4 (s)	518.5 511.4 502.4	502.9 (s)	515.4 (s)		δ_{M-C-O}
	513.2 (sh)		494.1 (sh)	510.6 (sh)		δ_{M-C-O}
	507.5 (w)			505.3 (w)		
	488.9 (br, m)		473.8 (br, m)	486.6 (br, m)		δ_{M-C-O}
	432.6 (w)		420.4 (w)	431.2 (w)		δ_{M-C-O}
	407.9 (m)	407.9 (m)	407.4 (m)	406.9 (m)		ν_{M-Cl}
	390.4 (s)	389.2 (s)	388.3 (s)	389.2 (s)		ν_{M-Cl}
	377.6 (sh)		380.5 (sh) 375.5 (sh)	377.3 (sh)		ν_{M-Cl}
trans-$[Ni(CO)_2Cl_2]$	522.8 (s)	522.6 515.9 508.1	508.6 (s)	520.4 (s)		δ_{M-C-O} (b_{1u})
	447.0 (w)			444.7 (w)		δ_{M-C-O} (b_{2u})
	428.2 (s)	425.7 (s)	425.5 (s)	428.4 (s)		ν_{M-Cl} (b_{1u})
	394.3 (m)	393.2 (m)	391.7 (m)	388.9 (m)		ν_{M-C} (b_{3u})
tet-$[Ni(CO)_2Cl_2]$	355.9 (s)	351.5 (s)	345.0 (s)	353.8 (s)		δ_{M-C-O}
	328.5 (s)	328.0 (s)	328.5 (s)	329.5 (s)		ν_{M-Cl}

[a] In cm^{-1}.

In the case of $CoCl_2$, after annealing there is a shoulder present (on the "free" CO band) at a frequency of ca. 2132 cm^{-1}. For $NiCl_2$ we were not able to assign any new bands after annealing except possibly at 2160 cm^{-1}, the region 2140–2160 cm^{-1} being largely obscured.

B. Pure Carbon Monoxide Matrices (or Argon Matrices Highly Enriched with Carbon Monoxide). (i) $FeCl_2$. The results of studying the isolation of $FeCl_2$ in pure carbon monoxide using infrared spectroscopy coupled with isotopic substitution are given in Table III, no annealing being necessary in this case. The data can be interpreted unambiguously using a *trans*-$[Fe(CO)_4Cl_2]$ D_{4h} molecule. Figure 1 summarizes the various isotopic experiments and, in the case of the 1:1 mixture of $^{12}CO/^{13}CO$, identifies the a_{2u} (quintet) and e_u (triplet) modes associated with these two infrared active δ_{MCO} vibrations. (Although the higher frequency δ_{MCO} mode of Figure 1c superficially looks like a triplet, the peak to peak spacings correspond to a quintet. The outermost pure ^{12}CO and pure ^{13}CO peak positions are too weak to be seen in the mixed isotope experiment but are identified in parts b and d of Figure 1.) The two δ_{MCO} modes shift by ca. 15 cm^{-1} for ^{13}CO substitution and ca. 2 cm^{-1} for $C^{18}O$ substitution (see Table III). A complex band near 385 cm^{-1} in the natural CO matrix contains ν_{M-Cl} at ca. 387 cm^{-1} and ν_{M-C} at 380 cm^{-1}. This latter band is identified by the shift of 6.6 cm^{-1} on $C^{18}O$ substitution but 5.4 cm^{-1} on ^{13}CO substitution. The ν_{M-C} mode is close to that observed by Pankowski and Bigorne[12] in *trans*-$[Fe(CO)_4I_2]$ at ca. 413 cm^{-1}. Bennett and Clark[23] assigned the ν_{Fe-Cl} modes in *cis*-$[Fe(CO)_4Cl_2]$ at 294 and 310 cm^{-1}, approximately 80 cm^{-1} lower than our assignment of the trans species. Two factors contribute to this difference: (a) the ClFeCl angle will be ca. 90° for the cis compound, which (on an SVFF model for a triatomic molecule) leads to the frequency being lowered by ca. 10% (35 cm^{-1}) for a constant force constant; (b) in the case of the cis compound, Cl is trans to CO leading to a further lowering in frequency relative to trans-$[Fe(CO)_4Cl_2]$.

An X-ray absorption spectroscopic study (XAS) was carried out on $FeCl_2$ isolated in carbon monoxide using the iron K-edge.[24] Figure 2a shows the extended X-ray absorption fine structure (EXAFS) obtained by background subtraction from the raw experimental data. The frequency of the oscillations (which arise from a summation of damped sine waves) is dependent on the interatomic distances from the iron atom, correlated with phase shift terms arising from the photoelectron interacting with the atomic potential of the iron and its neighbors. The amplitude (damping) of the oscillations is determined by the following: the number, atom type, and distance of the surrounding backscatterers; thermal and static disorder (Debye–Waller factor, $2\sigma^2$); lifetime of the final state and photoelectron mean free path (VPI); and processes such as shake up and shake off that do not contribute to the EXAFS (AFAC). In the case of $[Fe(CO)_4Cl_2]$, the corresponding Fourier transform (Figure 2b) gives *approximately* the distances between the central iron atom and C, Cl, and O successively. It is not possible to determine interatomic distances solely from the Fourier transform because of phase shift terms, so that a least-squares refinement procedure is employed. A feature to note in the Fourier transform is the intensity enhancement of the oxygen shell due to the focusing effect of the carbon atom in linear or near linear systems, and this has been modeled using curved wave multiple scattering theory including

(19) Seanor, D. A.; Amberg, C. H. *J. Chem. Phys.* **1965**, *42*, 2967–2970. Albers, D.; Colville, N. J.; Ford, T. A.; Hall, M. V. M.; Levendis, D. C. *Spectrochim. Acta* **1989**, *45A*, 249–252. Hush, N. S.; Williams, M. L. *J. Mol. Spectrosc.* **1974**, *50*, 349–368. Morterra, C.; Garrone, E.; Bolis, V.; Fubini, B. *Spectrochim. Acta* **1987**, *43A*, 1577–1581. Bolis, V.; Fubini, B.; Garrone, E.; Morterra, C. *J. Chem. Soc., Faraday Trans. 1* **1989**, *85*, 1383–1395. Platero, E. E.; Scarano, D.; Spoto, G.; Zecchina, A. *Faraday Discuss. Chem. Soc.* **1985**, *80*, 183–193.

(20) Dubost, H.; Abouaf-Marguin, L. *Chem. Phys. Lett.* **1972**, *17*, 269–273.

(21) Andrews, L.; Arlinghaus, R. T.; Johnson, G. L. *J. Chem. Phys.* **1983**, *78*, 6347–6352. Altman, R. S.; Marshall, M. D.; Klemperer, W.; Krupnov, A. *J. Chem. Phys.* **1983**, *79*, 52–56.

(22) Dubost, H. *Chem. Phys.* **1976**, *12*, 139–151. Dubost, H.; Lecuyer, A.; Charneau, R. *Chem. Phys. Lett.* **1979**, *66*, 191–194.

(23) Bennett, M. A.; Clark, R. J. H. *J. Chem. Soc.* **1964**, 5560–5568.

(24) For a general introduction to EXAFS in matrices, see: Beattie, I. R.; Binsted, N.; Levason, W.; Ogden, J. S.; Spicer, M. D.; Young, N. A. *High Temp. Sci.* **1990**, *26*, 71–86.

Table IV. Refined EXAFS Parameters[a]

	r_{M-C}/Å[b]	$2\sigma^2_{M-C}$/Å^{2}[c]	r_{M-O}/Å	$2\sigma^2_{M-O}$/Å^2	r_{M-Cl}/Å	$2\sigma^2_{M-Cl}$/Å	E_0/eV	VPI/eV	AFAC	FI[d]	R[e]
$[Fe(CO)_4Cl_2]$[f]	1.850 (2)	0.0054 (5)	2.959 (3)	0.0098 (4)	2.255 (2)	0.0028 (3)	26.8 (3)	−3.0	0.74	8.76	30.01
$[Cr(CO)_4Cl_2]$[f]	2.001 (3)	0.0071 (6)	3.106 (3)	0.0123 (5)	2.266 (2)	0.0060 (4)	23.5 (3)	−4.5	0.84	5.83	30.07
$[Fe(CO)_5]$[f]	1.796 (1)	0.0028 (3)	2.917 (2)	0.0077 (2)			27.5 (2)	−3.0	0.74	5.51	17.85
electron diffraction[27]	1.822 (3)		2.967 (4)								
X-ray diffraction[28,29]	1.82 (2)		2.95 (3)								
	1.79 (2)		2.91 (3)								
$[Cr(CO)_6]$[f]	1.892 (2)	0.0041 (3)	3.018 (2)	0.0086 (3)			28.0 (3)	−4.5	0.84	9.43	27.92
electron diffraction[35]	1.92 (4)		3.08 (5)								
X-ray diffraction[36]	1.916 (3)		3.087 (4)								
neutron diffraction[37]	1.918 (3)		3.059 (4)								

[a] Standard deviation in parentheses. [b] Estimated systematic errors are ±1.5% for well-defined coordination shells.[26] [c] $2\sigma^2$ is the Debye–Waller factor. [d] $FI = \sum_i\{(\chi_i^T(k) - \chi_i^E(k))(k^3)\}^2$. [e] $R = [\int k^n|(\chi^T(k) - \chi^E(k))|\,dk / \int k^n|(\chi^E(k))|\,dk] \times 100$. [f] This work.

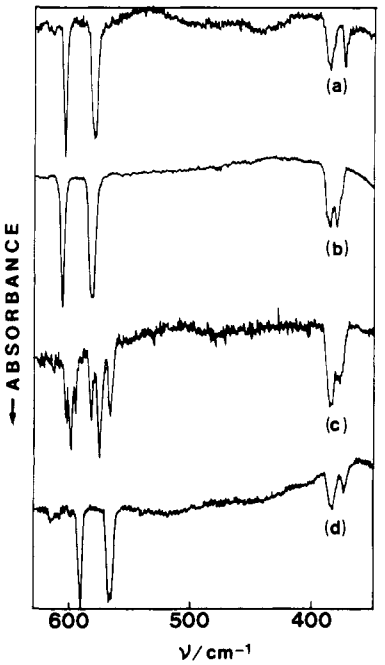

Figure 1. Infrared spectra of $FeCl_2$ isolated in carbon monoxide matrices: (a) $^{12}C^{18}O$; (b) $^{12}C^{16}O$; (c) $^{12}C^{16}O$:$^{13}C^{16}O$ ~1:1; (d) $^{13}C^{16}O$.

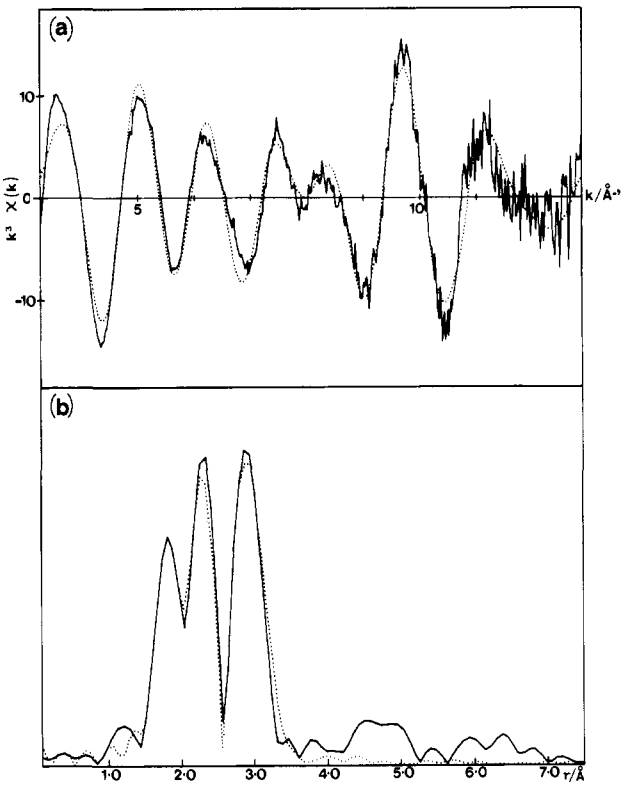

Figure 2. (a) EXAFS spectra and (b) Fourier transforms for $FeCl_2$ isolated in solid carbon monoxide: (—) experiment; (···) curved wave multiple scattering theory for $[Fe(CO)_4Cl_2]$.

up to third-order scattering contributions. Higher order multiple scattering was not included as it has been shown previously[25] that "we can be sure that a multiple scattering theory including contributions up to third order will be adequate in describing molecular structure..."; similarly, scattering paths between ligands were not included because[25] "it is apparent that the inter ligand paths are of much less importance...and could in general be neglected except in close-packed structures". For the Fe–Cl distances, single scattering curved wave theory was employed. The use of curved wave theory as opposed to plane wave theory enables analysis of data much nearer the edge (ca. 14 eV in this case) where multiple scattering contributions are strong.

The theoretical fit in Figure 2 has been calculated for $[Fe(CO)_4Cl_2]$ using the above approach, together with an Fe–C–O bond angle of 180°, and the data are included in Table IV. The systematic errors arising from data collection and analysis have been estimated[26] to be ±1.5% for well-defined coordination shells, and it can be seen that these are an order of magnitude above the statistical errors from the refinement process. Also included in this table are the data obtained by us for $[Fe(CO)_5]$ at 9 K together with the literature values from electron diffraction[27] and X-ray diffraction studies.[28,29] The agreement for these is satisfactory, and the discrepancy is smaller than that obtained by Binsted et al.[30] for $[Fe_2(CO)_9]$ and $[Fe_3(CO)_{12}]$, indicating that the phase shift and backscattering factors are satisfactory. $[Fe(CO)_5]$ was studied to act as a "calibrant" for the number of carbonyl ligands in the $FeCl_2$/CO complex. (AFAC was set at 0.74 by comparison with an iron metal foil.) To determine the optimum value of VPI for a carbonyl occupancy of 5, a correlation map of Debye–Waller factor (for the Fe–C shell) and VPI was calculated, and this gave a well-defined minimum at VPI = −3.0 eV. To check that this was a real minimum, a series of refinements using this value were carried out by varying the CO occupation number between 0.5 and 8 in steps of 0.5, and this confirmed that the minimum in the fit index was indeed at five carbonyl ligands. To determine the number of carbonyl ligands in $[Fe(CO)_nCl_2]$ a similar approach was used with VPI = −3.0 eV, and the result of this is shown in Figure 3, indicating that there are four carbon monoxides and thus confirming the presence of $[Fe(CO)_4Cl_2]$. The correlations between the refined parameters and especially the amplitude terms were well within acceptable limits, i.e., <0.8. Although the relatively large values of E_0 (ca. 26 eV) are equivalent to an energy about 10 eV below the muffin tin zero (−15.7 eV), they are in the expected range for metal carbonyl systems.[25]

For $[Fe(CO)_4Cl_2]$ the Fe–C and Fe–O distances are ca. 0.05 and 0.04 Å longer respectively than the corresponding values found

(25) Binsted, N.; Cook, S. L.; Evans, J.; Greaves, G. N.; Price, R. J. *J. Am. Chem. Soc.* **1987**, *109*, 3669–3676.
(26) Corker, J. M.; Evans, J.; Leach, H.; Levason, W. *J. Chem. Soc., Chem. Commun.* **1989**, 181–183.
(27) Beagley, B.; Cruickshank, D. W. J.; Pinder, P. M.; Robiette, A. G.; Sheldrick, G. M. *Acta Crystallogr.* **1969**, *B25*, 737–744.
(28) Hanson, A. W. *Acta Crystallogr.* **1962**, *15*, 930–933.
(29) Donohue, J.; Caron, A. *Acta Crystallogr.* **1964**, *17*, 663–667.
(30) Binsted, N.; Evans, J.; Greaves, G. N.; Price, R. J. *J. Chem. Soc., Chem. Commun.* **1987**, 1330–1333.

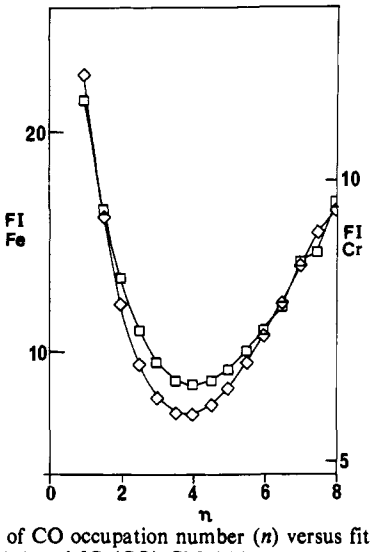

Figure 3. Plot of CO occupation number (n) versus fit index (FI) for $[Fe(CO)_nCl_2]$ (□) and $[Cr(CO)_nCl_2]$ (◇).

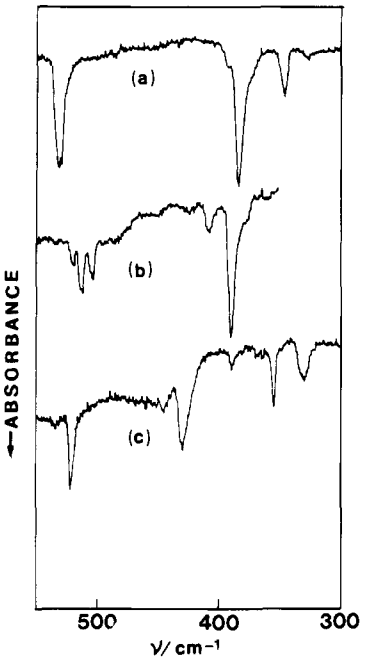

Figure 4. Infrared spectra of metal dichlorides isolated in carbon monoxide matrices: (a) $CrCl_2/^{12}C^{18}O$; (b) $CoCl_2/^{12}C^{16}O$:$^{13}C^{16}O$ ~1:1; (c) $NiCl_2/^{12}C^{18}O$.

for $[Fe(CO)_5]$ (where we were unable to differentiate axial and equatorial bonds from the high-quality spectrum). The Fe–Cl bond length of 2.25 (3) Å is shorter than that of the analogous iron(II) phosphine $Fe(VPP)_2Cl_2$ (VPP = *cis*-1,2-bis(diphenylphosphino)ethylene) by ca. 0.11 Å for the high-spin form and ca. 0.08 Å for the low-spin form.[31]

(ii) $CrCl_2$. The infrared spectrum of $CrCl_2$ in pure carbon monoxide shows characteristic δ_{MCO} and ν_{M-C} modes, indicating the formation of a carbonyl halide (see Table IV and Figure 4a). Unfortunately, in this case, there appear to be two overlapping bands in the δ_{MCO} region so that it is not possible to ascertain the number of carbon monoxide ligands by mixed $^{12}CO/^{13}CO$ partial isotopic enrichment. Cr(II) is a d^4 system, and either square planar (frequently with further interactions) or octahedral species are known.[32] In view of the fact that the matrix is pure ligand, the most likely species is *trans*-$[Cr(CO)_4Cl_2]$, directly analogous to

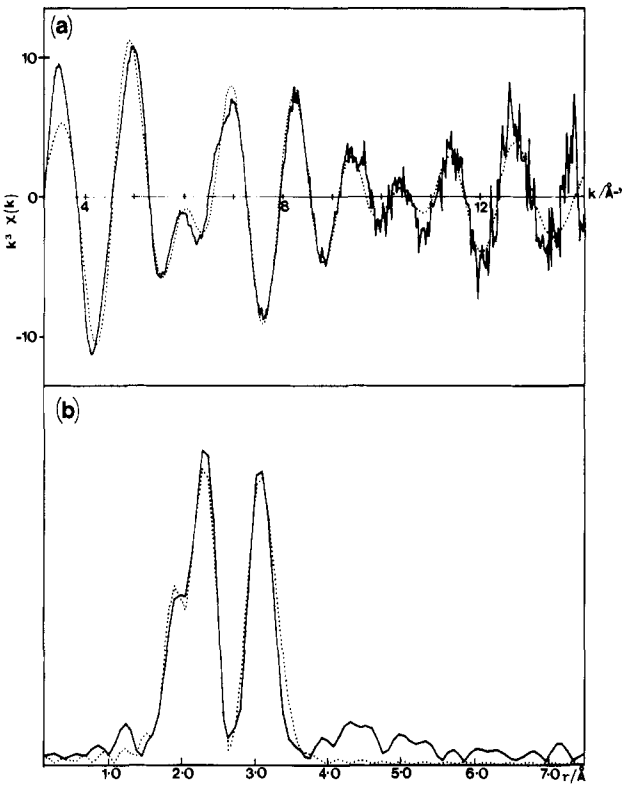

Figure 5. (a) EXAFS spectra and (b) Fourier transforms for $CrCl_2$ isolated in solid carbon monoxide: (—) experiment; (···) curved wave multiple scattering theory for $[Cr(CO)_4Cl_2]$.

the iron compound but with only 16 electrons. The related compound of molybdenum of empirical formula $[Mo(CO)_4Cl_2]$ has been reported,[33] but is now known to be dimeric with a metal–metal bond. In view of the excellent agreement between the XAS and infrared data for *trans*-$[Fe(CO)_4Cl_2]$ it seemed likely that the number of carbonyl groups in the chromium case might be defined by EXAFS. Figure 5a,b shows the EXAFS and corresponding Fourier transform for $CrCl_2$ isolated in a carbon monoxide matrix (after appropriate background subtraction). In order to "calibrate" the CO occupation number and determine a value for VPI, the same approach as that used for the iron case was employed with $[Cr(CO)_6]$ as the reference compound. AFAC was set at 0.84 as determined previously[34] for a Cr metal foil. By variation of VPI with a fixed occupation number of 6, a value of −4.5 eV was found to be the optimum. The refined parameters for $[Cr(CO)_6]$ at 9 K are collected in Table IV, together with those from previous electron,[35] X-ray,[36] and neutron diffraction[37] studies. The agreement is good, indicating that the phase shift and backscattering factors for Cr–C and Cr–O are satisfactory. Those for Cr–Cl have been validated in a previous experiment on CrO_2Cl_2 isolated in a nitrogen matrix.[34]

From the refinements at various occupation numbers for $CrCl_2$/CO (Figure 3) it is clear that the CO occupation is 4 as in the iron case. The theoretical curve in Figure 5 is that calculated for $[Cr(CO)_4Cl_2]$ using curved wave multiple scattering (including up to third order for the CO units). The Cr–C and Cr–O distances are longer than those for $[Cr(CO)_6]$ by ca. 0.11 and 0.09 Å, respectively. The Cr–Cl bond length (2.27 (3) Å) is shorter than that in the analogous low-spin phosphine *trans*-$[CrCl_2(dmpe)_2]$[38] by ca. 0.08 Å (dmpe = 1,2-bis(dimethylphosphino)ethane).

(31) Cecconi, F.; Di Vaira, M.; Midollini, S.; Orlandini, A.; Sacconi, L. *Inorg. Chem.* **1981**, *20*, 3423–3430.
(32) See, for example: Jubb, J.; Larkworthy, L. F.; Povey, D. C.; Smith, G. W. *Polyhedron* **1989**, *8*, 1825–1826. Ladd, M. F. C.; Larkworthy, L. F.; Leonard, G. A.; Povey, D. C.; Tandon, S. S. *J. Chem. Soc., Dalton Trans.* **1984**, 2351–2352. Hermes, A. R.; Girolami, G. S. *Inorg. Chem.* **1988**, *27*, 1775–1781.
(33) Colton, R.; Tomkins, I. B. *Aust. J. Chem.* **1966**, *19*, 1143–1146.
(34) Spicer, M. D.; Young, N. A. *J. Chem. Soc., Dalton Trans.* **1991**, 3133–3135.
(35) Brockway, L. O.; Ewens, R. V. G.; Lister, M. W. *Trans. Faraday Soc.* **1938**, *34*, 1350–1357.
(36) Whitaker, A.; Jeffery, J. W. *Acta Crystallogr.* **1967**, *23*, 977–984.
(37) Jost, A.; Rees, B.; Yelon, W. B. *Acta Crystallogr.* **1975**, *B31*, 2649–2658.
(38) Girolami, G. S.; Wilkinson, G.; Galas, A. M. R.; Thornton-Pett, M.; Hursthouse, M. B. *J. Chem. Soc., Dalton Trans.* **1985**, 1339–1348.

A *combination* of infrared and EXAFS data thus leads to the conclusion that the species present in the matrix is *trans*-[$Cr(CO)_4Cl_2$].

The Cr–Cl and Fe–Cl bond distances in the *trans*-[$M(CO)_4Cl_2$] species are similar (2.27 and 2.25 Å, respectively). However, there is a difference of 0.15 Å in the M–C distances, the chromium again giving the greater bond length. The iron compound is expected to be low spin. The lack of a substantial tetragonal distortion for the chromium compound agrees[39] with a low-spin configuration, which would also be favored by the low temperature[40] (ca. 9 K) at which the spectroscopies were carried out.

(iii) $CoCl_2$ and $NiCl_2$. By analogy with (a) the behavior of nickel(II) halides with phosphines to give "complexes", usually of the type [$Ni(PR_3)_2X_2$],[41] and (b) the formation of planar *cis*- or *trans*-[$Pt(CO)_2Cl_2$],[42] we might expect *linear* $NiCl_2$ to interact with carbon monoxide to yield the diamagnetic species *trans*-[$Ni(CO)_2Cl_2$]. However, the results shown in Table III and Figure 4c indicate that the system $NiCl_2$–carbon monoxide is more complicated than this. We therefore carried out infrared spectroscopic studies of $NiCl_2$ in CO/argon mixtures at successively increasing concentrations of carbon monoxide. The bands at 355.9 (δ_{MCO} mode) and 328.5 cm^{-1} (Ni–Cl stretch) were only seen at concentrations above ca. 50% carbon monoxide. As "tetrahedral" complexes of $NiCl_2$ with tertiary phosphines give ν_{M-Cl} in the region of 320 cm^{-1}, it is likely that it is the form of [$NiCl_2(CO)_2$] which is responsible for the 328.5-cm^{-1} band.[43] If the vapor from the subliming $NiCl_2$ was heated to a higher temperature (ca. 620 °C) than in a normal matrix isolation experiment, the two lower frequency bands were relatively more intense, but decreased in intensity on annealing.

A trans formulation for the species showing ν_{M-Cl} at 428.2 cm^{-1} is in agreement with *trans*-[$NiCl_2(PH_3)_2$] showing[43] ν_{M-Cl} above 400 cm^{-1}. In the δ_{MCO} region, the sharp band at 522.8 cm^{-1} becomes a clear triplet (ca. 1:2:1) in a 1:1 ^{12}CO:^{13}CO matrix and there is no indication of another δ_{MCO} mode under this band. We therefore assume that this is the in-plane b_{1u} mode of *trans*-[$Ni(CO)_2Cl_2$], which can couple with the infrared active ν_{M-Cl} antisymmetric stretch. Again, this is in agreement with a D_{2h} formulation, but does not exclude D_{4h} (see section 2). There is possibly another (weak) δ_{MCO} mode near 450 cm^{-1} which would be assigned to the out-of-plane mode of b_{2u} symmetry (here z is taken as the ClNiCl direction, and y is perpendicular to the molecular plane).

For $CoCl_2$ in carbon monoxide the spectra were complex (Figure 4b) and suggested the presence of at least two species. $CoCl_2$ is a d^7 system so that addition of more than three carbonyl groups in a low-spin configuration would place an electron in a high-energy orbital. Unfortunately, in this case, studies using varying ratios of Ar:CO in the matrices did not distinguish the various species present. Four δ_{MCO} modes are observable, the two weak ones (507.5 and 513.2 cm^{-1}) being of variable intensity and increasing on annealing. A ν_{M-Cl} mode at 377.6 cm^{-1} was also of variable intensity and increased on annealing. The most intense δ_{MCO} mode becomes a triplet (ca. 1:2:1) in a 1:1 ^{12}CO:^{13}CO matrix, indicating the presence of two or four carbonyl groups in D_{2h} or D_{4h} symmetry, respectively, and excluding a trigonal bipyramidal D_{3h} structure with three carbonyl groups. The frequencies of the two main bands, 518.4 and 390.4 cm^{-1}, are close to those of *trans*-[$Cr(CO)_4Cl_2$] at 533.8 and 384.3 cm^{-1}, suggesting that the major species is *trans*-[$Co(CO)_4Cl_2$]. Appealing to the chemistry of rhodium and iridium does not help as we are not aware of any carbonyl halides of these metals in the +2 oxidation state.

Because of the presence of more than one species in the matrix for $CoCl_2$ and $NiCl_2$, any EXAFS data would not be capable of rigorous interpretation. In particular, square planar and tetrahedral configurations lead to different electronic properties, each giving rise to a set of EXAFS oscillations with a different origin.

(iv) $CaCl_2$, $MnCl_2$, and $ZnCl_2$. For $CaCl_2$ (d^0), $MnCl_2$ (d^5), and $ZnCl_2$ (d^{10}) no ^{12}CO- or ^{13}CO-sensitive modes were observed. However, in all cases, there were substantial changes in the M–Cl stretching frequencies (given below in cm^{-1}) from those in a pure argon matrix.

$$\text{Ca: } 402\ (\text{Ar}) \rightarrow 325\ (\text{CO})$$

$$\text{Mn: } 477\ (\text{Ar})^{14a} \rightarrow 375\ (\text{CO})$$

$$\text{Zn: } 510\ (\text{Ar})^{44} \rightarrow 410\ (\text{CO})$$

No isotopic data could be obtained as the bands were broad and featureless.

From previous work,[1] it is known that the earlier transition metal dichlorides show a relatively small change in force constant between argon and nitrogen matrices. However, there is a progressive increase from manganese to nickel which shows a dramatic (>30%) change in force constant.[1,6] By contrast, zinc shows a behavior similar to that of the earlier members, giving a change of some 10%. In many ways, the behavior of $ZnCl_2$ in CO is similar to that of $NiCl_2$ in nitrogen. Calculations by DeKock et al.[45] on the interaction of CaF_2 with CO suggest that, for these dichlorides, the primary interaction between the metal atom and the carbon monoxide molecule will be via the carbon. The most probable explanation is then that $ZnCl_2$ is nonlinear in a CO matrix, giving the formation of a (weak) tetrahedral adduct. It is unclear if this is due to ion-induced dipole interactions or if there is also a significant contribution from charge-transfer interactions. The broadness of bands in CO could be associated with the asymmetry of the molecule coupled with a range of Cl–Zn–Cl and M–C–O angles, unlike the 180° metal–carbonyl angles expected for the carbonyl halides. Finally, it is interesting to recall that Zn^{II} is isoelectronic with Cu^{I}, for which there are well-established carbonyl species.[46]

4. Conclusions

The investigations carried out here demonstrate the formation of *trans*-[$Fe(CO)_4Cl_2$], *trans*-[$Cr(CO)_4Cl_2$], and *trans*-[$Ni(CO)_2Cl_2$]. They also show that $CaCl_2$, $MnCl_2$, and $ZnCl_2$ interact strongly with carbon monoxide, probably mainly via ion-induced dipole interactions. In the case of $CoCl_2$, more than one species is present in the matrix and the only certain feature is that carbonyl halides are formed.

The position of ν_{CO} (cm^{-1}) in these metal carbonyl halides follows the sequence Cr (2096), Fe (2111), Co (2132), Ni (2160), the last two frequencies being open to question. However, it is the expected trend from "$\pi \rightarrow \sigma$" interaction with the CO.

The above observations are in line with what might have been predicted from a general knowledge of the chemistry of carbon monoxide in association with metal centers. However, there are two additional features of interest. One of these is that CO can interact with $CrCl_2$ or $FeCl_2$ either to give a van der Waals species or to form a carbonyl halide. The other is that there appears to be a critical situation in which a metal dichloride molecule can interact with its surroundings with a minor perturbation (e.g., $ZnCl_2$ in N_2, $NiCl_2$ in Ar) or with a major reorganization (e.g., $ZnCl_2$ in CO, $NiCl_2$ in N_2). These observations may be of considerable importance in understanding catalytic processes involving CO on metal oxide surfaces, for example.

5. Experimental Section

Materials. $CaCl_2$ (Aldrich 99.99%), $MnCl_2 \cdot 4H_2O$ (BDH Analar), or $CoCl_2 \cdot 6H_2O$ (BDH Analar) was dried at ca. 120 °C, followed by heating

(39) Jubb, J.; Larkworthy, L. F.; Oliver, L. F.; Povey, D. C.; Smith, G. W. *J. Chem. Soc., Dalton Trans.* **1991**, 2045–2050

(40) Halepoto, D. M.; Holt, D. G. L.; Larkworthy, L. F.; Leigh, G. J.; Povey, D. C.; Smith, G. W. *J. Chem. Soc., Chem. Commun.* **1989**, 1322–1323. Halepoto, D. M.; Holt, D. G.; Larkworthy, L. F.; Povey, D. C.; Smith, G. W.; Leigh, G. J. *Polyhedron* **1989**, *8*, 1821–1822.

(41) See, for example: Levason, W. In *The Chemistry of Organophosphorus Compounds*, Hartley, F. R., Ed.; Wiley: New York, 1990; pp 567–641.

(42) Dell Amico, D. B.; Calderazzo, F.; Veracini, C. A.; Zandana, N. *Inorg. Chem.* **1984**, *23*, 3030–3033. Browning, J.; Goggin, P. L.; Goodfellow, R. J.; Norton, M. G.; Rattray, A. J. M.; Taylor, B. F.; Mink, J. *J. Chem. Soc., Dalton Trans.* **1977**, 2061–2067.

(43) Boorman, P. M.; Carty, A. J. *Inorg. Nucl. Chem. Lett.* **1968**, *4*, 101–105.

(44) Millington, K. R. Ph.D. Thesis, University of Southampton (U.K.), 1987.

(45) DeKock, R. L.; Remington, R. B.; Schaefer, H. F. Unpublished work.

(46) See, for example: Desjardins, C. D.; Edwards, D. B.; Passmore, J. *Can. J. Chem.* **1979**, *57*, 2714–2715.

in vacuo at ca. 250 °C. The dichlorides of chromium and zinc (and occasionally nickel) were prepared from the reaction of high-purity metals (Goodfellow) with AgCl in an argon atmosphere, using a metal:AgCl ratio of approximately 10:1. The tube containing the reactants was then evacuated so that the dichloride could be sublimed away from the metal and sealed off for storage. For the synthesis of $Cr^{37}Cl_2$, isotopic $Ag^{37}Cl$ was prepared from enriched $Na^{37}Cl$ (Monsanto 95% ^{37}Cl). $FeCl_2$ and $NiCl_2$ were prepared from the reaction of high-purity metal wire or foil with HCl (gas) (BDH 99.6%). Matrix gases were as follows: high-purity argon (BOC 99.998%), carbon monoxide (BOC research grade 99.95%), ^{13}CO (Amersham International 99% ^{13}C), and $C^{18}O$ (Bureau des Isotopes Stable 97% ^{18}O).

Matrix Isolation Infrared Spectroscopy. The anhydrous or sublimed materials were transferred to a conventional matrix isolation apparatus[47] equipped with a silica dome and radio frequency (in the case of $CaCl_2$) or resistive heating. Sample deposition times were typically 1 h, and the vapors were cocondensed with a large excess of matrix gas onto a CsI window held at 8-9 K by a closed cycle refrigerator (APD Cryogenics DE204SL). Sublimation temperatures for the dichlorides followed the expected trend across the series and were *approximately* as follows (°C): Ca, 900; Cr, 650; Mn, 520; Fe, 450; Co, 450; Ni, 450; Zn, 300. Infrared spectra were recorded in the region 4000-200 cm^{-1} using a purged Perkin-Elmer PE983G spectrometer operating normally at a resolution of 0.65 cm^{-1} and calibrated using water vapor. Spectral manipulations were carried out with a PE 3600 data station.

Matrix Isolation X-ray Absorption Experiments. For the EXAFS matrix isolation experiments, the techniques used[24] were similar to those described above except that (a) the central window was aluminum (Goodfellow 99.995%) and (b) deposition was monitored by observing the increase in the absorption edge (typical time 4-5 h). In order to mask fluorescence due to metal impurities in the aluminum, the window was pretreated with a thin film of krypton (for the chromium studies) or argon (for the iron studies). X-ray absorption spectra were measured in the fluorescence mode using an Ar/He-filled ion chamber (Cr, 15 Torr of Ar; Fe, 24 Torr of Ar) to monitor I_0 and a Tl-doped NaI crystal scintillator to monitor I_f. Typically, six to eight spectra were recorded and averaged.

The data were collected on station 8.1 of the SERC Daresbury Laboratory Synchrotron Radiation Source (SRS) using Si[111] or Si[220] order sorting double crystal monochromators at 50% harmonic rejection and a platinum focusing mirror. The SRS operated at 2 GeV with beam currents in the range 200-300 mA, and data were collected at the metal K-edges. Background subtraction was carried out using PAXAS[48] by fitting the preedge region to a quadratic polynomial and subtracting this function from the whole spectrum. The atomic component of the oscillatory part of the spectrum was approximated using high-order (typically six) polynomials and optimized by minimizing the chemically insignificant shells ($r < 1$ Å) in the Fourier transform. Curve fitting utilized the curved wave theory in the SERC Daresbury Laboratory EXCURVE90 program.[49] Phase shifts and backscattering factors were calculated by the usual ab initio methods[49] and found to be satisfactory without further modification.

Acknowledgment. We thank Miss Ingrid Fussing, Mr. Mark Keeble, and particularly Mr. A. D. Willson for preliminary work. Dr. P. Goggin provided original infrared and Raman spectra while Professor H. F. Schaefer sent us a manuscript prior to publication. We thank Professor J. Evans and Dr. W. Levason for many helpful discussions; Drs. W. Levason, J. S. Ogden, and particularly M. D. Spicer for help with the synchrotron experiments; and the Science and Engineering Research Council (U.K.) and AEA Technology, Winfrith (U.K.), for financial support. We also thank the Director of Daresbury Laboratory for experimental and computational facilities.

(47) Beattie, I. R.; Jones, P. J.; Millington, K. R.; Willson, A. D. *J. Chem. Soc., Dalton Trans.* **1988**, 2759-2762.

(48) Binsted, N. *PAXAS, Program for the Analysis of X-ray Absorption Spectra*; University of Southampton (U.K.), 1988.

(49) Gurman, S. J., Binsted, N., Ross, I. *J. Phys. C* **1984**, *17*, 143-151; **1986**, *19*, 1845-1861.

Dehydrogenation of Ethylene and Propylene and Ethylene Polymerization Induced by Ti^+ in the Gas Phase

B. C. Guo and A. W. Castleman, Jr.*

Contribution from the Department of Chemistry, The Pennsylvania State University, University Park, Pennsylvania 16802. *Received January 9, 1992*

Abstract: The chemistry of multiple-step reactions of Ti^+ with ethylene and propylene was examined using a SIDT-LV apparatus (selected ion drift tube with laser vaporization source) at thermal energies. Bare Ti^+ exhibits an active dehydrogenation reactivity toward the alkene molecules. However, the coordination of ligands on Ti^+ dramatically alters its dehydrogenation reactivity. For propylene, the multiple-step reactions virtually terminate at the fourth step, whereas the reactions with ethylene molecules go far beyond the fourth step. Over 20 ethylene molecules, thus far, have been observed to react with Ti^+, whereupon their products attach to Ti^+. On the basis of various experimental results, we believe that a large number of ethylene molecules attaching onto a bare Ti^+ at room temperature indicates that the polymerization of ethylene induced by Ti^+ has occurred in the gas phase and that the polymerization process follows essentially the same mechanism by which olefin polymerization catalyzed by Ziegler-Natta catalysts proceeds in the condensed phase. According to the basic concepts of Cossee's theory, we have developed a simple model to interpret the findings. The model suggests that titanacyclobutane is formed in a six-coordinated Ti(I) complex to initiate the ethylene polymerization. Then, more ethylene molecules will coordinate onto the vacant coordinating site of Ti^+, followed by the interposition of the coordinated ethylene from Ti^+ to the alkyl group. The reaction patterns are indicative of a continuing stepwise mechanism leading to the formation of a larger and larger ethylene polymer.

1. Introduction

One of the most exciting and far-reaching discoveries in chemistry over the past 40 years is the use of transition metal complex catalysts for alkene and diene polymerization. It was Ziegler and Natta who discovered the so-called Ziegler-Natta catalyst in the 1950's which made a revolutionary change in the modern rubber and plastics industry.[1,2] Since then, vast amounts of research in this area have been carried out by both industrial and academic scientists. The research ranges from the development of new high-activity industrial catalysts to fundamental research.[3-6] As a result, the Ziegler-Natta catalyst has been continuously upgraded to improve the commercial production of olefin polymers.

(1) Ziegler, K.; Holzkampf, E.; Breil, H.; Martin, H. *Angew. Chem.* **1955**, *67*, 541.

(2) Natta, G. *J. Polym. Sci.* **1955**, *16*, 143.

(3) *Transition metals and Organometallics as Catalysts for Olefin Polymerization*; Kaminsky, W., Sinn, H., Eds.; Springer Verlag: Berlin, 1987.

(4) *Transition Metal Catalyzed Polymerizations*; Quirk, R. P., Ed.; Cambridge University Press: Cambridge, 1988.

(5) *Catalytic Olefin Polymerization*; Keij, T., Soga, K., Eds.; Elsevier: New York, 1990.

(6) *Transition Metal Catalyzed Polymerization*; Quirk, R. P., Ed.; MMI Press: Harwood, 1983.

0002-7863/92/1514-6152$03.00/0